






Article

Nickolayite, FeMoP, a new natural molybdenum phosphide

Mikhail N. Murashko¹, Sergey N. Britvin^{1,2*} , Yevgeny Vapnik³, Yury S. Polekhovskiy^{1,†}, Vladimir V. Shilovskikh⁴ , Anatoly N. Zaitsev¹ and Oleg S. Vereshchagin¹ 

¹Institute of Earth Sciences, Saint-Petersburg State University, Universitetskaya Nab. 7/9, St. Petersburg, 199034, Russia; ²Nanomaterials Research Center, Kola Science Center, Russian Academy of Sciences, Fersman Str. 14, Apatity, 184200, Russia; ³Department of Geological and Environmental Sciences, Ben-Gurion University of the Negev, POB 653, Beer-Sheva, 84105, Israel; and ⁴Geomodel Resource Center, Saint-Petersburg State University, Ulyanovskaya Str. 1, St. Petersburg, 198504, Russia

Abstract

Nickolayite, FeMoP, is a new terrestrial phosphide structurally related to allabogdanite (high-pressure modification of (Fe,Ni)₂P), and the meteoritic phosphides florenskyite, FeTiP and andreiyvanovite, FeCrP. From the point of view of chemical composition, nickolayite is an Fe-analogue of monipite, MoNiP. The mineral was discovered in the Daba-Siwaqa complex, Central Jordan, a part of the pyrometamorphic Hatrurim Formation (the Mottled Zone), whose outcrops encompass a 150 × 200 km area around the Dead Sea in the Middle East. Nickolayite appears as an accessory phase in the fused clinopyroxene–plagioclase rocks texturally resembling gabbro–dolerite. The irregularly shaped grains of the mineral, up to 80 μm in size are associated with baryte, tridymite, chromite, hematite, pyrrhotite, fluorapatite, titanite and powellite. Macroscopically, nickolayite grains possess light-grey to greyish-white colour and metallic lustre. The mineral is ductile. The mean VHN hardness (50 g load) is 538 kg mm⁻². The calculated density based on the empirical formula and the unit-cell parameters is 7.819 g cm⁻³. In reflected light, nickolayite has a white colour, with no bireflectance or pleochroism. The COM approved reflectance values [*R*_{max}/*R*_{min} (%), λ(nm)] are: 48.5/46.5 (470), 50.5/48.5 (546), 51.8/49.9 (589) and 53.9/52.0 (650). The chemical composition of the holotype crystal is (electron microprobe, average of 4 analyses, wt.%): Fe 32.21, Mo 47.06, Ni 3.69, Co 0.13, P 17.45, total 100.54, that corresponds to the empirical formula Fe_{1.00}(Mo_{0.87}Ni_{0.11}Fe_{0.02})Σ_{1.00}P_{1.00} and an ideal formula of FeMoP. Nickolayite is orthorhombic, space group *Pnma*, unit-cell parameters of holotype material are: *a* = 5.9519(5), *b* = 3.7070(3), *c* = 6.8465(6) Å, *V* = 151.06(2) Å³ and *Z* = 4. The crystal structure of holotype material was solved and refined to *R*₁ = 0.0174 based on 251 unique observed reflections. The origin of the mineral is probably connected to the processes of co-reduction of molybdenum- and phosphorus-bearing minerals during high-temperature pyrometamorphic processes.

Keywords: phosphide, molybdenum, crystal structure, pyrometamorphism, gabbro–dolerite, Dead Sea, Middle East, Hatrurim Formation

(Received 19 February 2022; accepted 18 May 2022; Accepted Manuscript published online: 30 May 2022; Associate Editor: Michael Rumsey)

Introduction

The Hatrurim Formation, often referred to as the Mottled Zone, is the world's largest pyrometamorphic complex (Gross, 1977). The term 'pyrometamorphism' incorporates a suite of natural processes and environments which can provide high-temperature and low-pressure calcination and fusion of sedimentary lithologies (Grapes, 2011). The typical case is calcination of sediments entrapped by (or in contact with) igneous rocks (Reverdatto, 1970; Clark and Peacor, 1992; Souza *et al.*, 2019). When the high-temperature processes are maintained at the expense of burning organic matter (bitumen, coal), the term 'combustion metamorphism' is often used (Grapes, 2011). Due to the inherently spatial nature, pyrometamorphism is preferentially a local

phenomenon confined, e.g. to volcanic eruptions, subsurface magmatic chambers or natural coal fires (Burnham, 1959; Grapes, 2011). The Hatrurim Formation is a rare exception, as the eroded remnants of the Mottled Zone can be traced across an area of 150 × 200 km around the Dead Sea, both in Israel and Jordan (Gross, 1977; Burg *et al.*, 1992). The unprecedented scale of the Hatrurim Formation leads to the appearance of various pyrometamorphic lithologies with diverse mineral assemblages (Sharygin *et al.*, 2008; 2021; Murashko *et al.*, 2011; Galuskin *et al.*, 2015; Sokol *et al.*, 2019; Khoury, 2020; Juroszek *et al.*, 2020; Britvin *et al.*, 2021a). Natural terrestrial phosphides are one such unique feature of these rare mineral assemblages (Britvin *et al.*, 2015). The majority of phosphides discovered in the Hatrurim Formation belong to the system Fe–Ni–P (Britvin *et al.*, 2017a; 2019a,b; 2020a,b,c; 2022a). However, recent exploration has discovered a series of molybdenum-bearing phosphides (Britvin *et al.*, 2022b). In this paper, we describe a new mineral, FeMoP, discovered on the Jordanian side of the Hatrurim Formation. The mineral has been named nickolayite, in honour of Dieter Nickolay (born 1941), the German mineral collector

*Author for correspondence: Sergey N. Britvin, Email: sergei.britvin@spbu.ru

†Deceased 29 September 2018

Cite this article: Murashko M.N., Britvin S.N., Vapnik Y., Polekhovskiy Y.S., Shilovskikh V.V., Zaitsev A.N. and Vereshchagin O.S. (2022) Nickolayite, FeMoP, a new natural molybdenum phosphide. *Mineralogical Magazine* 86, 749–757. <https://doi.org/10.1180/mgm.2022.52>



Fig. 1. The dark green–grey paralava schlieren, along with white calcite veinlets dissecting metamorphosed chalk. Phosphorite quarry, Daba Siwaqa complex, West Jordan.

and mineralogist, for his contributions to the studies in systematic mineralogy. Dieter Nickolay studied mineralogy at the University of Freiburg in 1983; he is a member of the German mineral collectors' community (VFMG) and one of the volunteers involved in preparation and verification of *The New IMA List of Minerals* (Pasero, 2022). Both the mineral and its name (symbol Nkl) have been approved by the Commission on New Minerals, Nomenclature and Classification (CNMNC) of the International Mineralogical Association (IMA2018-126, Murashko *et al.*, 2019). The holotype specimen of nickolayite is deposited in the collections of the Fersman Mineralogical Museum of the Russian Academy of Sciences, Moscow, Russia, with the registration number 5290/1.

Materials and methods

Thick polished sections containing nickolayite were prepared from the cut rock slices using conventional preparation techniques. The reflected-light study included visual description and reflectivity measurements performed in air by means of a MSF-2 spectrophotometer (LOMO, St. Petersburg), using Si as a reference material. After an optical investigation, the sections were coated with carbon film and underwent electron microprobe

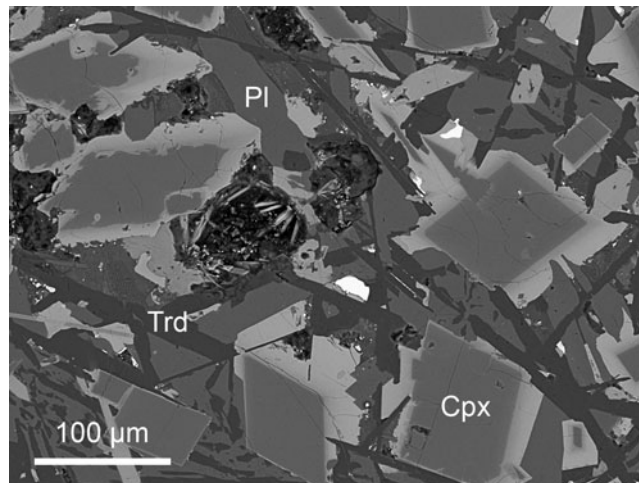


Fig. 2. The microstructure of nickolayite-bearing paralava. The cross-sections of euhedral clinopyroxene crystals (Cpx) exhibit sharp compositional zoning in back-scattered electrons (BSE), due to differences in Fe/Mg contents (cf. Table 2). Plagioclase (Pl) (Table 1) and tridymite (Trd), along with pyrrhotite (white inclusions) fill up the interstices between clinopyroxene crystals. Polished section, SEM BSE image.

analysis, using an INCA WAVE 500 WDX spectrometer (20 kV, 15 nA) attached to a Hitachi S-3400N scanning electron microscope (SEM). Pure Ni, Fe and Co metals ($K\alpha$ lines) and InP ($PK\alpha$) were used as analytical standards. The analyses of rock-forming minerals were completed using the same instrumental setup, with oxides and silicates as reference standards. The microhardness measurements were performed after completion of microprobe studies, following the extraction of selected nickolayite grains for the X-ray examination.

The single-crystal X-ray studies of the holotype crystal were carried out using a four-circle Bruker APEX Kappa DUO CCD diffractometer equipped with a $MoK\alpha$ microfocus tube, operated at 50 kV and 0.6 mA. A single-crystal X-ray dataset for the low-Mo nickolayite was obtained by means of Bruker Smart APEX CCD diffractometer equipped with a $MoK\alpha$ tube, operated at 50 kV and 40 mA. Data collection and unit-cell refinements were performed with the Bruker APEX2 software package (Bruker Inc.), whereas subsequent data reduction and integration procedures were carried out with *CrysAlisPro v. 171.41* software (Rigaku Oxford Diffraction, 2021). The crystal structure was solved and refined by the *SHELX-2018* set of programs (Sheldrick, 2015) incorporated into the *Olex2 v.1-5* graphical user interface (Dolomanov *et al.*, 2009). The details of data collection, reduction, structure solution and refinement can be retrieved from the crystallographic information files (CIF) which are included in the supplementary information. Powder X-ray diffraction data for the holotype material were obtained from the same grain that was used for the structure refinement, using a Gandolfi method implemented at the Rigaku RAXIS Rapid II imaging plate diffractometer. The instrument setup was as follows: $CoK\alpha$ radiation (rotating anode) with microfocus mirror optics, 40 kV, 15 mA, curved (semi-cylindrical) imaging plate ($r = 128.4$ mm), Debye-Scherrer geometry and exposure 60 mn. The data-to-profile conversion was performed using *osc2xrd* software (Britvin *et al.*, 2017b). Unit-cell parameters refinement and calculation of theoretical pattern was carried out with *STOE WinXPow v.2.08* software (Stoe & Cie GmbH).

Table 1. Representative chemical compositions of anorthite associated with nickolayite (wt.%).*

#	1	2	3	4	5
CaO	19.40	18.67	18.24	17.99	17.66
Na ₂ O	0.49	0.75	0.71	0.75	0.85
K ₂ O	0.40	0.50	0.39	0.43	0.65
MgO	b.d.l.	b.d.l.	b.d.l.	b.d.l.	b.d.l.
Al ₂ O ₃	32.71	32.24	32.69	32.39	31.35
Fe ₂ O ₃	1.41	1.52	1.47	1.59	1.50
SiO ₂	45.68	46.69	46.60	47.15	48.15
Total	100.09	100.37	100.10	100.30	100.16
Formula based on O = 8 atoms per formula unit					
Ca	0.97	0.92	0.90	0.89	0.87
Na	0.04	0.07	0.06	0.07	0.08
K	0.02	0.03	0.02	0.03	0.04
Σ	1.03	1.02	0.99	0.98	0.99
Si	2.12	2.16	2.15	2.17	2.22
Al	1.79	1.76	1.78	1.76	1.70
Fe	0.05	0.05	0.05	0.06	0.05
Σ	3.96	3.97	3.98	3.99	3.97

*b.d.l. – below detection limit

Results

Occurrence and mineral assemblages

Nickolayite was found in a small quarry operated for phosphorites, located in the Jizah District, Amman Governorate, Jordan (31°21'52"N, 36°10'55"E) (Britvin *et al.*, 2015). The quarry exposes a suite of pyrometamorphic rocks belonging to the Hatrurim Formation, in general comprising severely metamorphosed chalks and marls. Phosphide assemblages, described previously, are confined to the fused, originally sedimentary lithologies, known in the literature under the term 'paralava' (Vapnik *et al.*, 2007) (Fig. 1). The paralavas containing nickolayite are dense rocks of dark-brown colour, consisting of submillimetre-sized elongated crystals of clinopyroxene and anorthite (Fig. 2). The mineral composition and texture of these paralavas resembles that of gabbro–dolerites, but they exhibit

some specific features, such as a spatially high content of tridymite (confirmed by electron back-scatter diffraction - EBSD). Plagioclase crystals are chemically homogeneous and show compositions within a narrow range of Na/Ca ratios, approaching an anorthite end-member (Table 1). In contrast, the clinopyroxenes exhibit an extraordinary compositional zonation, varying from diopside (core) to hedenbergite (rim) within the same crystal (Table 2, Fig. 1) and can contain considerable amounts of Cr, V and Ti (Table 2). In addition, clinopyroxene can contain considerable amounts of Cr, V and Ti (Table 2). The accessory minerals are represented by baryte, chromite, hematite, trevorite, pyrrhotite, fluorapatite, titanite and powellite. The paralavas bear numerous submillimetre- to millimetre-sized cavities typically filled with secondary calcite (Fig. 1).

Appearance and physical properties of nickolayite

Nickolayite forms irregularly shaped rounded single-crystal grains up to 80 µm, disseminated in the host silicate matrix (Fig. 3). The grains show no signs of alteration (reaction) at the contact with the rock-forming minerals. In reflected light, the mineral has a purely white colour with no observable birefringence or pleochroism. It exhibits very weak anisotropy ($\Delta R_{589} = 1.95\%$). Reflectance values are presented in Table 3. Loose nickolayite grains extracted from the rock matrix have metallic light-grey to greyish-white colour. The mineral is ductile and has no cleavage. The mean micro-indentation hardness (VHN load of 50 g) is 538 mm⁻², ranging from 490 to 588 kg mm⁻², which corresponds to a Mohs hardness of 5 to 6. The density of the holotype crystal calculated from the empirical formula and the single-crystal unit-cell parameters is 7.840 g cm⁻³.

Chemical composition

The composition of three nickolayite grains was investigated (Table 4). The individual grains are homogeneous, with no chemical zoning. However, each one differs significantly in

Table 2. Representative chemical compositions of clinopyroxene associated with nickolayite (wt.%).*

#	1	2	3	4	5	6	7	8	9
Zone	core	rim	rim	rim	core	core	core	core	rim
CaO	24.81	23.46	22.99	22.33	23.12	22.52	23.39	23.15	22.09
MgO	17.65	7.35	4.15	1.19	6.40	4.98	6.12	2.99	0.74
FeO	1.42	17.98	22.20	26.56	16.80	17.20	18.73	24.99	28.30
Al ₂ O ₃	0.97	1.41	1.30	1.27	2.59	3.44	2.24	1.30	1.51
V ₂ O ₃	b.d.l.	b.d.l.	b.d.l.	b.d.l.	1.21	1.95	b.d.l.	b.d.l.	b.d.l.
Cr ₂ O ₃	b.d.l.	b.d.l.	b.d.l.	b.d.l.	1.92	2.59	1.45	b.d.l.	b.d.l.
TiO ₂	b.d.l.	b.d.l.	b.d.l.	1.33	b.d.l.	b.d.l.	b.d.l.	1.15	1.09
SiO ₂	55.31	49.99	49.40	47.31	47.90	47.26	48.10	46.37	46.42
Total	100.16	100.19	100.04	99.99	99.94	99.94	100.03	99.95	100.15
Formula calculated on the basis of Σ=4 cations per formula unit									
Ca	0.96	0.98	0.98	0.98	0.98	0.96	0.99	1.00	0.97
Mg	0.95	0.43	0.25	0.07	0.38	0.30	0.36	0.18	0.05
Fe ²⁺	0.04	0.59	0.74	0.91	0.55	0.57	0.62	0.85	0.97
Al	0.04	0.06	0.06	0.06	0.12	0.16	0.10	0.06	0.07
V ³⁺					0.02	0.03			
Cr					0.06	0.08	0.05		
Ti				0.04				0.03	0.03
Si	2.00	1.95	1.97	1.94	1.89	1.89	1.89	1.87	1.91
O	6.02	5.98	6.00	6.01	5.99	6.03	5.97	5.94	5.98

*b.d.l. – below detection limit

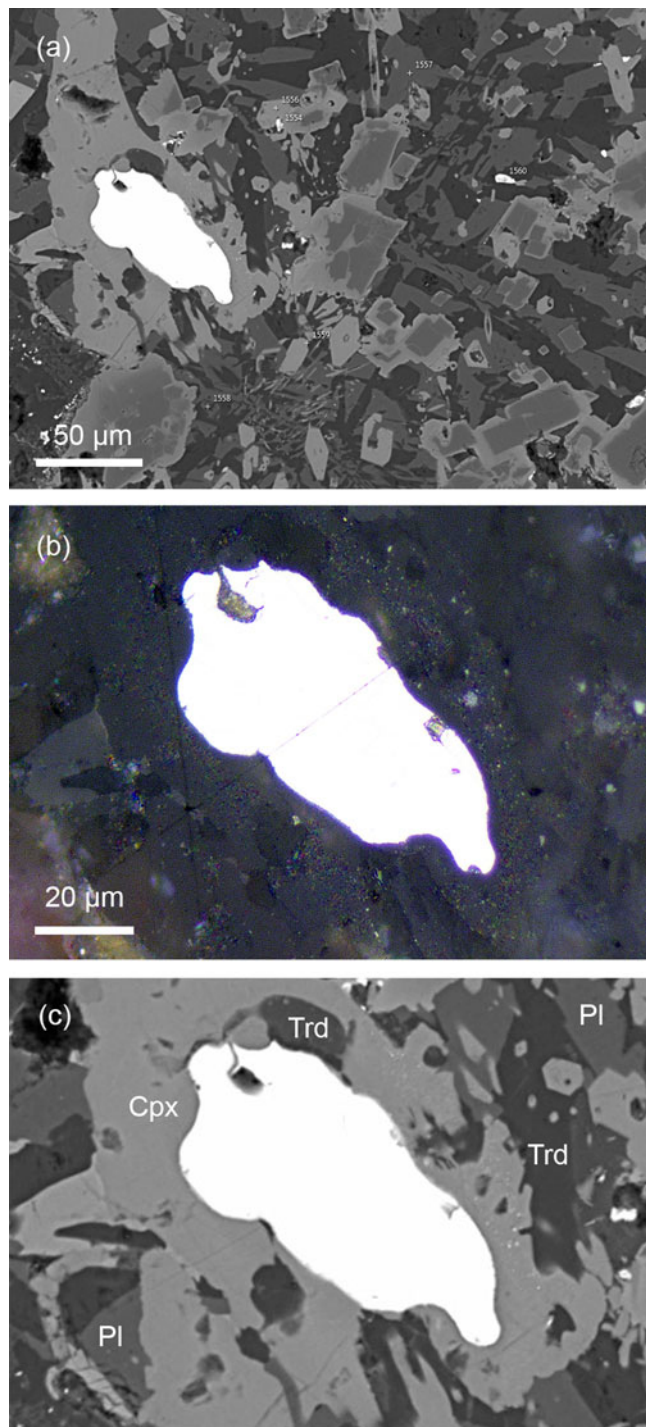


Fig. 3. The holotype nickolayite grain (specimen number 5290/1) in paralava. (a) General view. (b, c) The enlarged area, photomicrograph in reflected light (b) and BSE image (c). Abbreviations: Cpx – clinopyroxene; Trd – tridymite; and Pl – plagioclase.

composition from the other two. The holotype crystal (#1 in Table 4) has the highest Mo content (0.87 atoms per formula unit), whereas grain #3 is depleted in Mo (0.44 Mo apfu) and, from the formal point of view, represents a composition intermediate between nickolayite, FeMoP, and Mo-rich allabogdanite, (Fe,Mo)₂P (Fe>Mo). The crystal structure determinations

Table 3. Reflectance values for nickolayite (%).*

R_{\max}	R_{\min}	λ (nm)	R_{\max}	R_{\min}	λ (nm)
46.9	44.7	400	50.9	49.0	560
47.4	45.2	420	51.5	49.6	580
47.8	45.7	440	51.8	49.9	589
48.2	46.2	460	52.2	50.2	600
48.5	46.5	470	52.9	50.9	620
48.8	46.7	480	53.6	51.6	640
49.2	47.3	500	53.9	52.0	650
49.8	47.7	520	54.2	52.3	660
50.4	48.3	540	54.8	52.9	680
50.5	48.5	546	55.6	53.6	700

*Data for wavelengths recommended by the IMA Commission on ore microscopy (COM) are marked in boldtype.

performed for grains #1 and #3 (see below) confirm the results of electron microprobe analyses. The plot of the chemical compositions presented in Fig. 4 reveals that the change in the Mo contents linearly and inversely correlates with the change in the Fe contents, implying the substitution of 1 Fe atom for 1 Mo atom. At the same time, the Ni concentration remains almost constant: a feature which cannot be explained on the basis of the available data.

Crystal structure and powder X-ray diffraction

X-ray structural studies were carried out on crystal #1 (the holotype one) and #3 (for the compositions, see Table 4). Their crystal parameters, data collection and structure refinement details are given in Table 5; atomic coordinates and thermal displacement parameters are listed in Table 6. Nickolayite, being an analogue of synthetic FeMoP, belongs to the structural type TiNiSi – a metal-ordered variant of the Co₂Si framework (Rundqvist and Nawapong, 1966; Guérin and Sergent, 1977). As a consequence, the nickolayite structure (Fig. 5) has the same site geometry and lattice metrics as the structure of the only known natural Co₂Si-type phosphide, allabogdanite (Britvin *et al.*, 2002). There are two symmetrically independent metal sites: *M*(1), tetrahedrally coordinated by 4 phosphorus atoms, and *M*(2), which is five-fold coordinated by P, resulting in square–pyramidal coordination (Fig. 5). Phosphorus, is nine-fold coordinated by both metal and P atoms. The corner- and edge-sharing [*M*(1)P₄] and [*M*(2)P₅] polyhedra are arranged into infinite chains propagated along the *b* axis (Fig. 5). Both metal sites allow wide homogeneity ranges, where, in particular, Mo can be substituted by either Fe or Ni (Rundqvist and Nawapong, 1966; Guérin and Sergent, 1977; Oliynyk *et al.*, 2013).

The nickolayite crystals studied are distinguished by significantly different Mo contents; therefore they are of interest in view of Mo distribution across the structure. The free refinements of site populations reveal that Mo only incorporates into the square–pyramidal *M*(2) site. Taking into account that the atomic metal radius of Mo (1.39 Å) is greater than the corresponding radii of Fe and Ni (1.26 and 1.24 Å, respectively) (Pauling, 1960), the observed behaviour agrees well with the longer *M*–P distances at the *M*(2) site, in contrast to the considerably shorter *M*(1)–P bonds (Table 7). In addition, the *M*(2)–P bonds in the Mo-rich crystal #1 are longer than the corresponding bonds in the Mo-poor crystal #3 (Table 7). However, our data disagrees with the random distribution of Mo and Fe over the *M*(1) and *M*(2) sites as was determined in the synthetic

Table 4. Chemical composition of nickolayite (wt.%).

	#1 (n = 4) *	Range (S.D.)	#2 (n = 6)	Range (S.D.)	#3 (n = 5)	Range (S.D.)
Fe	32.21	31.83–32.77 (0.42)	44.35	43.75–44.79 (0.46)	49.90	49.58–50.39 (0.34)
Co	0.13	0.11–0.17 (0.03)	0.16	0.13–0.18 (0.02)	0.20	0.17–0.24 (0.03)
Ni	3.69	3.63–3.73 (0.05)	3.51	3.32–3.70 (0.14)	3.79	3.69–3.90 (0.09)
Mo	47.06	46.18–47.78 (0.69)	33.41	32.79–34.27 (0.61)	26.11	25.78–26.29 (0.20)
P	17.45	17.21–17.77 (0.23)	18.08	17.94–18.19 (0.11)	19.26	19.03–19.49 (0.20)
Total	100.54		99.50		99.26	
Formula	$\text{Fe}_{1.00}(\text{Mo}_{0.87}\text{Ni}_{0.11}\text{Fe}_{0.02})_{1.00}\text{P}_{1.00}$		$\text{Fe}_{1.00}(\text{Mo}_{0.58}\text{Fe}_{0.33}\text{Ni}_{0.10})_{1.01}\text{P}_{0.98}$		$\text{Fe}_{1.00}(\text{Mo}_{0.44}\text{Fe}_{0.44}\text{Ni}_{0.10}\text{Co}_{0.01})_{0.99}\text{P}_{1.01}$	

*The holotype material; S.D. – standard deviation.

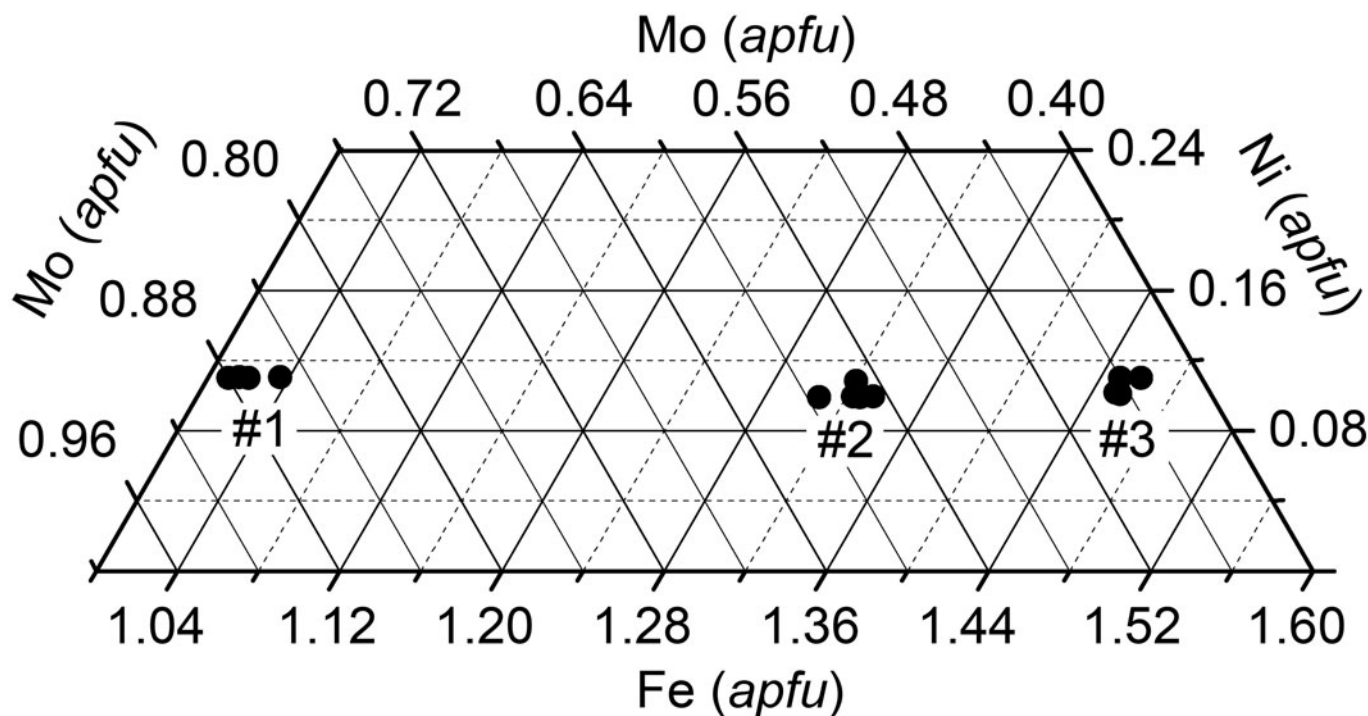


Fig. 4. Part of the Fe–Mo–Ni ternary diagram illustrating the chemical composition of the nickolayite crystals studied.

$(\text{Mo}_{1-x}\text{Fe}_x)_2\text{P}$ solid solutions (Oliynyk *et al.*, 2013). This discrepancy between natural nickolayite and synthetic $(\text{Mo}_{1-x}\text{Fe}_x)_2\text{P}$ may indicate that in the latter case, the synthesis time was insufficient for completion of the diffusion processes, so the metal site ordering seen in nickolayite was not achieved (*cf.* Britvin *et al.*, 2021c). The free occupancy refinements of the $M(1)$ site show that the latter is populated solely by Fe. Nickel is thus incorporated into the $M(2)$ position, leading to the structural formulae given in Table 5, which are consistent with the microprobe data (Table 4).

Powder X-ray diffraction data for crystal #1 are given in Table 8. The unit-cell parameters refined from the XRD pattern are: $a = 5.942(1)$, $b = 3.703(1)$, $c = 6.841(2)$ Å and $V = 150.52(4)$ Å³.

Discussion

Relationship to other phosphides and arsenides

Nickolayite is the second terrestrial Mo-bearing phosphide, after polekhovskiyite, MoNiP_2 (Britvin *et al.*, 2022a). The mineral expands the series of natural phosphides belonging to the

NiTiSi or Co_2Si structure type (Table 9). From the chemical point of view, nickolayite is an Fe analogue of monipite, MoNiP (Ma *et al.*, 2014) (Table 9). However, the latter crystallises in the barringerite structure type (the low-pressure hexagonal Fe_2P) (Buseck, 1969; Carlsson *et al.*, 1973), and its synthetic analogue is not known to adopt the Co_2Si structure type (Guérin and Sergent, 1977). With the exception of nickolayite, all minerals listed in Table 9 were originally discovered in meteorites. Allabogdanite, the high-pressure modification of $(\text{Fe,Ni})_2\text{P}$ (Britvin *et al.*, 2019c), has been described recently in terrestrial pyrometamorphic rocks of the Hatrurim Formation in Israel (Britvin *et al.*, 2021b), however the others remain solely of meteoritic origin. Besides phosphides, two arsenide minerals belong to the Co_2Si structure type: these are rhodarsenide, $(\text{Rh,Pd})_2\text{As}$ (Tarkian *et al.*, 1997), and palladodymite, $(\text{Pd,Rh})_2\text{As}$ (Britvin *et al.*, 1999).

Some remarks on the origin of nickolayite

The enrichment in Mo minerals is a known feature of pyrometamorphic lithologies of the Hatrurim Formation. Since the 1960s it

Table 5. Crystal parameters, data collection and structure refinement details for nickolayite.

	Holotype crystal (#1)	Low-Mo crystal (#3)
Crystal parameters		
Structural formula	Fe(Mo _{0.88} Ni _{0.12})P	Fe(Mo _{0.45} Fe _{0.45} Ni _{0.10})P
Crystal size (mm)	0.04 × 0.02 × 0.01	0.05 × 0.05 × 0.03
Crystal system	Orthorhombic	Orthorhombic
Space group	<i>Pnma</i>	<i>Pnma</i>
<i>a</i> (Å)	5.9519(5)	5.8544(6)
<i>b</i> (Å)	3.7070(3)	3.6241(4)
<i>c</i> (Å)	6.8465(6)	6.7182(7)
<i>V</i> (Å ³)	151.06(2)	142.54(3)
<i>Z</i>	4	4
<i>D_x</i> (g cm ⁻³)	7.840	7.502
Data collection and refinement		
Instrument	Bruker Kappa APEX DUO	Bruker Smart APEXII
Radiation	MoKα (λ = 0.71073 Å)	MoKα (λ = 0.71073 Å)
Temperature (K)	296	296
2θ max (°)	truncated at 60.00	truncated at 60.00
Total reflections collected	3338	952
No. unique reflections	251	235
No. unique observed, <i>I</i> ≥ 2σ(<i>I</i>)	251	205
<i>h</i> , <i>k</i> , <i>l</i> range	−8→8, −5→5, −9→9	−8→8, −4→4, −9→5
<i>F</i> (000)	325	298
μ (mm ⁻¹)	18.77	20.42
No. refined parameters	20	19
<i>R</i> _{int} , <i>R</i> _σ	0.0374, 0.0113	0.0275, 0.0240
<i>R</i> ₁ [<i>F</i> ≥ 4σ(<i>F</i>)], <i>R</i> ₁ (all data)	0.0174, 0.0174	0.0224, 0.0293
<i>wR</i> ₂ *	0.0435	0.0402
<i>S</i> = GoF	1.136	1.144
Largest diff. peak / hole (e ⁻ Å ⁻³)	−0.99, 0.97	−1.20, 1.16

*SHELX weighting scheme applied: $w^{-1} = [\sigma^2(F_o^2) + (0.0255P)^2 + 0.5924P]$ (crystal #1); $w^{-1} = [\sigma^2(F_o^2) + (0.0203P)^2]$ (crystal #3), where $P = [(F_o^2 + 2F_c^2)/3]$.

Table 6. Fractional atomic coordinates and displacement parameters (Å²) for nickolayite.*

Site**	<i>x</i>	<i>y</i>	<i>z</i>	<i>U</i> _{iso}	<i>U</i> ¹¹	<i>U</i> ²²	<i>U</i> ³³	<i>U</i> ¹³
Crystal #1								
<i>M</i> (1) (4c)	0.64102(9)	¾	0.43729(8)	0.00477(18)	0.0047(3)	0.0061(3)	0.0035(3)	0.00035(18)
<i>M</i> (2) (4c)	0.02900(5)	¾	0.67160(5)	0.00459(17)	0.0044(2)	0.0068(2)	0.0026(2)	−0.00023(10)
P (4c)	0.26587(16)	¾	0.37739(15)	0.0057(2)	0.0052(4)	0.0066(4)	0.0053(5)	−0.0004(3)
Crystal #3								
<i>M</i> (1) (4c)	0.64222(12)	¾	0.43740(11)	0.00451(19)	0.0044(3)	0.0058(4)	0.0033(3)	0.0002(3)
<i>M</i> (2) (4c)	0.02847(9)	¾	0.66915(8)	0.00469(16)	0.0043(2)	0.0064(3)	0.0034(2)	−0.0001(2)
P (4c)	0.2640(2)	¾	0.37652(19)	0.0053(3)	0.0053(5)	0.0056(7)	0.0049(6)	−0.0008(5)

**U*¹² and *U*²³ displacement parameters are equal to zero owing to site symmetry.

**Occupancy of the *M*(1) site is Fe_{1.00} for both crystals. Occupancy of the *M*(2) site is Mo_{0.88}Ni_{0.12} (crystal #1) and Mo_{0.45}Fe_{0.45}Ni_{0.10} (crystal #3).

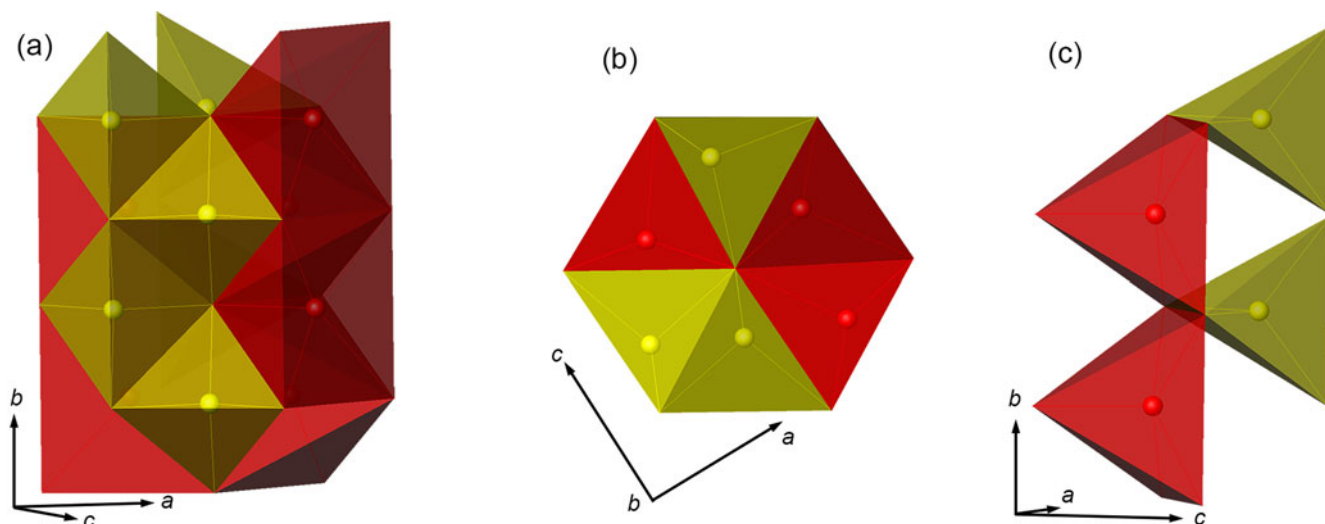


Fig. 5. Crystal structure of nickolayite. (a) General view along the *b* axis. Chains of edge- and corner-sharing tetrahedra [FeP₄] (yellow) and square pyramids [MoP₅] (red). (b) Projection onto (010) plane. (c) A fragment showing interconnections between tetrahedra [FeP₄] (yellow) and square pyramids [MoP₅] (red).

Table 7. Selected bond lengths (Å) in nickolayite.

	Crystal #1 M(1) = Fe	Crystal #2 M(1) = Fe
M(1)–P	2.2702(11)	2.2262(15)
M(1)–P	2.2790(11)	2.2518(15)
M(1)–P	2.3136(7) ×2	2.2689(9) ×2
M(2)–P	2.4587(10)	2.4013(15)
M(2)–P	2.5745(7) ×2	2.5118(10) ×2
M(2)–P	2.6289(7) ×2	2.5886(10) ×2

has been documented that the sedimentary strata – the protoliths of pyrometamorphic rocks – are enriched in Ni and Mo (Issar *et al.*, 1969; Ilani *et al.*, 1985; Gilat, 1994; Bogoch *et al.*, 1999; Ryb *et al.*, 2009; Fleurance *et al.*, 2013), and these elevated concentrations are retained in the marbles and paralavas of the Hatrum Formation. Powellite, CaMoO₄, an accessory mineral in the rocks of the Mottled Zone, was found both in Israel and Jordan (Khoury, 2020; Sokol *et al.*, 2020). Phosphides of the barringerite–transjordanite series, Fe₂P–Ni₂P, occurring on both sides of the Dead Sea, may contain up to 3 wt.% Mo (Britvin *et al.*, 2020a). Allabogdanite, the high-pressure modification of (Fe,Ni)₂P, also bears up to several wt.% Mo (Britvin *et al.*, 2021b). Prior to the discovery of nickolayite, the most Mo-rich

phosphide in this area was polekhovskiyite, MoNiP₂ with 44 wt.% Mo (Britvin *et al.*, 2022b). The likely pathway for the formation of Mo-bearing phosphides is co-reduction of oxygen-bearing Mo and Fe–Ni minerals and phosphates, which has been observed experimentally in corresponding synthetic systems (Burns *et al.*, 2007). Natural methane, hydrogen or bitumen are the likely candidates for the role of reductants (Novikov *et al.*, 2013; Galuskin *et al.*, 2020). The temperatures reached in pyrometamorphic processes (up to 1400°C) are more than sufficient for the initiation and maintenance of reduction reactions. Powellite might be a possible source of Mo. The accessory mineral, trevorite, NiFe₂O₄, could provide sufficient Ni supply, whereas fluorapatite is a widespread phosphate in the pyrometamorphic rocks of the Hatrum Formation. It is thus quite likely that nickolayite will not be the last Mo-phosphide discovered.

Acknowledgements. We are thankful to the Principal Editor Stuart Mills and Associate Editor Mike Rumsey for editorial handling and linguistic correction of the manuscript, and to Peter Leverett, the Structural Editor, for careful examination of crystallographic data. We are grateful to Igor Pekov and an anonymous referee for many valuable corrections and suggestions. This study was carried out with the financial support of the Russian Science Foundation, grant 18-17-00079. The authors thank the Centre for X-ray diffraction studies, Geomodel Resource Centre, and Centre of Microscopy and Microanalysis of St. Petersburg State University for the access to instrumental and computational resources.

Table 8. Powder X-ray diffraction data for holotype nickolayite (*d* in Å).*

<i>l</i> _{meas}	<i>d</i> _{meas}	<i>l</i> _{calc}	<i>d</i> _{calc}	<i>hkl</i>	<i>l</i> _{meas}	<i>d</i> _{meas}	<i>l</i> _{calc}	<i>d</i> _{calc}	<i>hkl</i>
		3	4.486	101	9	1.5017	11	1.5022	114
21	3.260	18	3.257	011	3	1.4964	8	1.4953	303
6	2.970	9	2.971	200	1	1.4851	3	1.4855	400
6	2.728	2	2.725	201	2	1.4524	4	1.4517	401
		27	2.317	210	3	1.4283	9	1.4279	222
100	2.316	100	2.314	112	19	1.3974	28	1.3971	123
10	2.243	14	2.243	202	2	1.3868	4	1.3866	313
84	2.196	87	2.195	211	2	1.3788	4	1.3787	410
25	2.128	41	2.129	103	2	1.3620	6	1.3626	402
13	1.9416	18	1.9417	013	3	1.3519	9	1.3515	411
5	1.9021	20	1.9025	301	3	1.3328	7	1.3333	105
15	1.8506	40	1.8515	020	10	1.3273	16	1.3269	321
		14	1.8457	113	2	1.2937	3	1.2939	223
3	1.8098	5	1.8089	203	4	1.2828	11	1.2834	015
8	1.7115	16	1.7140	302			5	1.2787	412
		5	1.7103	004	9	1.2575	16	1.2578	322
4	1.6255	2	1.6254	213			5	1.2563	024
3	1.5707	4	1.5713	220	3	1.2425	5	1.2428	205
3	1.5559	3	1.5555	312	6	1.2220	28	1.2220	314

*The theoretical pattern was calculated on the basis of atomic coordinates obtained from the structure refinement and unit-cell parameters refined from powder diffraction data. The intensities of seven strongest lines are highlighted in bold. Calculated lines with intensity <2 have been omitted.

Table 9. Comparative crystallographic data for nickolayite and some related minerals.

Mineral	Reference*	Formula	Structure type	Space group	<i>a</i> (Å)	<i>b</i> (Å)	<i>c</i> (Å)	<i>V</i> / <i>Z</i> (Å ³)	<i>Z</i>
Nickolayite	[1]	FeMoP	TiNiSi	<i>Pnma</i>	5.952	3.707	6.847	37.8	4
Florenskyite**	[2]	FeTiP	TiNiSi	<i>Pnma</i>	6.007	3.602	6.897	37.3	4
Andreyivanovite**	[3]	FeCrP	TiNiSi	<i>Pnma</i>	5.833	3.569	6.658	34.7	4
Allabogdanite	[4]	(Fe,Ni) ₂ P	Co ₂ Si	<i>Pnma</i>	5.792	3.564	6.691	34.5	4
Monipite**	[5]	MoNiP	Fe ₂ P	<i>P62m</i>	5.861		3.704	36.7	3

*References: [1] this work; [2] Ivanov *et al.* (2000), Rundqvist and Nawapong (1966); [3] Zolensky *et al.* (2008), Kumar *et al.* (2004); [4] Britvin *et al.* (2002); [5] Ma *et al.* (2014), Guérin and Sergent (1977).

**Structural data for natural florenskyite, andreyivanovite and monipite are not available; the unit cell parameters have been assigned on the basis of an EBSD pattern match with the corresponding synthetic analogues.

Supplementary material. To view supplementary material for this article, please visit <https://doi.org/10.1180/mgm.2022.52>

Competing interests. The authors declare that they have no conflict of interest.

References

- Bogoch R., Gilat A., Yoffe O. and Ehrlich S. (1999) Rare earth trace element distributions in the Mottled Zone complex, Israel. *Israel Journal of Earth Sciences*, **48**, 225–234.
- Britvin S.N., Rudashevsky N.S., Bogdanova A.N. and Shcherbachov D.K. (1999) Palladodymite (Pd,Rh)₂As, a new mineral from a glacier of the Miass River, the Urals. *Zapiski Rossiiskogo Mineralogicheskogo Obshchestva*, **128**, 104–107 [in Russian].
- Britvin S.N., Rudashevsky N.S., Krivovichev S.V., Burns P.C. and Polekhovskiy Yu.S. (2002) Allabogdanite, (Fe,Ni)₂P, a new mineral from the Onello meteorite: the occurrence and crystal structure. *American Mineralogist*, **87**, 1245–1249.
- Britvin S.N., Murashko M.N., Vapnik Ye., Polekhovskiy Yu.S. and Krivovichev S.V. (2015) Earth's phosphides in Levant and insights into the source of Archaean prebiotic phosphorus. *Scientific Reports*, **5**, 8355.
- Britvin S.N., Murashko M.N., Vapnik Ye., Polekhovskiy Yu.S. and Krivovichev S.V. (2017a) Barringerite Fe₂P from pyrometamorphic rocks of the Hatrurim Formation, Israel. *Geology of Ore Deposits*, **59**, 619–625.
- Britvin S.N., Dolivo-Dobrovolsky D.V. and Krzhizhanovskaya M.G. (2017b) Software for processing the X-ray powder diffraction data obtained from the curved image plate detector of Rigaku RAXIS Rapid II diffractometer. *Zapiski Rossiiskogo Mineralogicheskogo Obshchestva*, **146**, 104–107 [in Russian].
- Britvin S.N., Murashko M.N., Vapnik Ye., Polekhovskiy Yu.S., Krivovichev S.V., Vereshchagin O.S., Vlasenko N.S., Shilovskikh V.V. and Zaitsev A.N. (2019a) Zuktamrurite, FeP₂, a new mineral, the phosphide analogue of löllingite, FeAs₂. *Physics and Chemistry of Minerals*, **46**, 361–369.
- Britvin S.N., Vapnik Ye., Polekhovskiy Yu.S., Krivovichev S.V., Krzhizhanovskaya M.G., Gorelova L.A., Vereshchagin O.S., Shilovskikh V.V. and Zaitsev A.N. (2019b) Murashkoite, FeP, a new terrestrial phosphide from pyrometamorphic rocks of the Hatrurim Formation, Southern Levant. *Mineralogy and Petrology*, **113**, 237–248.
- Britvin S.N., Shilovskikh V.V., Pagano R., Vlasenko N.S., Zaitsev A.N., Krzhizhanovskaya M.G., Lozhkin M.S., Zolotarev A.A. and Gurzhiy V.V. (2019c) Allabogdanite, the high-pressure polymorph of (Fe,Ni)₂P, a stishovite-grade indicator of impact processes in the Fe–Ni–P system. *Scientific Reports*, **9**, 1047.
- Britvin S.N., Murashko M.N., Vapnik Ye., Polekhovskiy Yu.S., Krivovichev S.V., Krzhizhanovskaya M.G., Vereshchagin O.S., Shilovskikh V.V. and Vlasenko N.S. (2020a) Transjordanite, Ni₂P, a new terrestrial and meteoritic phosphide, and natural solid solutions barringerite–transjordanite (hexagonal Fe₂P–Ni₂P). *American Mineralogist*, **105**, 428–436.
- Britvin S.N., Murashko M.N., Vapnik Ye., Polekhovskiy Yu.S., Krivovichev S.V., Vereshchagin O.S., Shilovskikh V.V., Vlasenko N.S. and Krzhizhanovskaya M.G. (2020b) Halamishite, Ni₅P₄, a new terrestrial phosphide in the Ni–P system. *Physics and Chemistry of Minerals*, **2020**, 3.
- Britvin S.N., Murashko M.N., Vapnik Ye., Polekhovskiy Yu.S., Krivovichev S.V., Vereshchagin O.S., Shilovskikh V.V. and Krzhizhanovskaya M.G. (2020c) Negevite, the pyrite-type NiP₂, a new terrestrial phosphide. *American Mineralogist*, **105**, 422–427.
- Britvin S.N., Murashko M.N., Vapnik Ye., Vlasenko N.S., Krzhizhanovskaya M.G., Vereshchagin O.S., Bocharov V.N. and Lozhkin M.S. (2021a) Cyclophosphates, a new class of native phosphorus compounds, and some insights into prebiotic phosphorylation on early Earth. *Geology*, **49**, 382–386.
- Britvin S.N., Vereshchagin O.S., Shilovskikh V.V., Krzhizhanovskaya M.G., Gorelova L.A., Vlasenko N.S., Pakhomova A.S., Zaitsev A.N., Zolotarev A.A., Bykov M., Lozhkin M.S. and Nestola F. (2021b) Discovery of terrestrial allabogdanite (Fe,Ni)₂P, and the effect of Ni and Mo substitution on the barringerite–allabogdanite high-pressure transition. *American Mineralogist*, **106**, 944–952.
- Britvin S.N., Krzhizhanovskaya M.G., Zolotarev A.A., Gorelova L.A., Obolonskaya E.V., Vlasenko N.S., Shilovskikh V.V. and Murashko M.N. (2021c) Crystal chemistry of schreibersite, (Fe,Ni)₃P. *American Mineralogist*, **106**, 1520–1529.
- Britvin S.N., Murashko M.N., Krzhizhanovskaya M.G., Vereshchagin O.S., Vapnik Ye., Shilovskikh V.V., Lozhkin M.S. and Obolonskaya E.V. (2022a) Nazarovite, Ni₁₂P₅, a new terrestrial and meteoritic mineral structurally related to nickelposphide, Ni₃P. *American Mineralogist*, doi:10.2138/am-2022-8219.
- Britvin S.N., Murashko M.N., Vereshchagin O.S., Vapnik Ye., Shilovskikh V.V., Vlasenko N.S. and Permyakov V.V. (2022b) Expanding the speciation of terrestrial molybdenum: discovery of polekhovskiyite, MoNiP₂, and insights into the sources of Mo-phosphides in the Dead Sea Transform area. *American Mineralogist*, doi:10.2138/am-2022-8261.
- Burg A., Starinsky A., Bartov Y. and Kolodny Y. (1992) Geology of the Hatrurim Formation (“Mottled Zone”) in the Hatrurim basin. *Israel Journal of Earth Sciences*, **40**, 107–124.
- Burnham C.W. (1959) Contact metamorphism of magnesian limestones at Crestmore, California. *Bulletin of the Geological Society of America*, **70**, 879–920.
- Burns S., Hargreaves J.S.J. and Hunter S.M. (2007) On the use of methane as a reductant in the synthesis of transition metal phosphides. *Catalysis Communications*, **8**, 931–935.
- Buseck P.R. (1969) Phosphide from meteorites: barringerite, a new iron–nickel mineral. *Science*, **165**, 169–171.
- Carlsson B., Goelin M. and Rundqvist S. (1973) Determination of the homogeneity range and refinement of the crystal structure of Fe₂P. *Journal of Solid State Chemistry*, **8**, 57–67.
- Clark B.H. and Peacor D.R. (1992) Pyrometamorphism and partial melting of shales during combustion metamorphism: mineralogical, textural and chemical effects. *Contributions to Mineralogy and Petrology*, **112**, 558–568.
- Dolomanov O.V., Bourhis L.J., Gildea R.J., Howard J.A. and Puschmann H. (2009) OLEX2: a complete structure solution, refinement and analysis program. *Journal of Applied Crystallography*, **42**, 339–341.
- Fleurance S., Cuney M., Malartre M. and Reyx J. (2013) Origin of the extreme polymetallic enrichment (Cd, Cr, Mo, Ni, U, V, Zn) of the Late Cretaceous–Early Tertiary Belqa Group, central Jordan. *Palaeogeography, Palaeoclimatology, Palaeoecology*, **369**, 201–219.
- Galuskin E.V., Gfeller F., Galuskina I.O., Pakhomova A., Armbruster T., Vapnik Ye., Wlodzyka R., Dzierzanowski P. and Murashko M. (2015) New minerals with a modular structure derived from hatrurite from the pyrometamorphic Hatrurim Complex. Part II. Zadovite, BaCa₆[(SiO₄)(PO₄)](PO₄)₂F and aradite, BaCa₆[(SiO₄)(VO₄)](VO₄)₂F, from paravas of the Hatrurim Basin, Negev Desert, Israel. *Mineralogical Magazine*, **79**, 1073–1087.
- Galuskin E., Galuskina I., Vapnik Ye. and Murashko M. (2020) Molecular hydrogen in natural mayenite. *Minerals*, **10**, 560.
- Gilat A. (1994) Tectonic and associated mineralization activity, Southern Judea, Israel. *Geological Survey of Israel*, Report GSI/19/94, Jerusalem, 322 pp.
- Grapes R.H. (2011) *Pyrometamorphism* (2nd ed.). Springer Verlag, Berlin, 365 p.
- Gross H. (1977) The mineralogy of the Hatrurim Formation, Israel. *Geological Survey of Israel Bulletin*, **70**, 1–80.
- Guérin R. and Sergent M. (1977) Nouveaux arseniures et phosphures ternaires de molybdène ou de tungstène et d'éléments 3d, de formule: M_{2-x}Me_xX (M = élément 3d; Me = Mo, W; X = As, P). *Materials Research Bulletin*, **12**, 381–388.
- Ilani S., Kronfeld J. and Flexer A. (1985) Iron-rich veins related to structural lineaments, and the search for base metals in Israel. *Journal of Geochemical Exploration*, **24**, 197–206.
- Issar A., Eckstein Y. and Bogoch R. (1969) A possible thermal spring deposit in the Arad area, Israel. *Israel Journal of Earth Sciences*, **18**, 17–20.
- Ivanov A.V., Zolenskiy M.E., Saito A., Ohsumi K., MacPherson G.J., Yang S.V., Kononkova N.N. and Mikouchi T. (2000) Florenskiyite, FeTiP, a new phosphide from the Kaidun meteorite. *American Mineralogist*, **85**, 1082–1086.
- Juroszek R., Krüger B., Galuskina I., Krüger H., Vapnik Ye. and Galuskin E. (2020) Siwaqaite, Ca₆Al₂(CrO₄)₃(OH)₁₂·26H₂O, a new mineral of the ettringite group from the pyrometamorphic Daba-Siwaqa complex, Jordan. *American Mineralogist*, **105**, 409–421.
- Khoury H.N. (2020) High- and low-temperature mineral phases from the pyrometamorphic rocks, Jordan. *Arabian Journal of Geosciences*, **13**, 734.

- Kumar S., Krishnamurthy A., Bipin K., Srivastava K., Daa A. and Paranjpe S. (2004) Magnetization and neutron diffraction studies on FeCrP. *Pramana*, **63**, 199–205.
- Ma C., Beckett J.R. and Rossman G.R. (2014) Monipite, MoNiP, a new phosphide mineral in a Ca-Al-rich inclusion from the Allende meteorite. *American Mineralogist*, **99**, 198–205.
- Murashko M.N., Chukanov N.V., Mukhanova A.A., Vapnik E., Britvin S.N., Polekhovskiy Y.S. and Ivakin Y.D. (2011) Barioferrite BaFe₁₂O₁₉: A new mineral species of the magnetoplumbite group from the Hatrurim Formation in Israel. *Geology of Ore Deposits*, **53**, 558–563.
- Murashko M.N., Vapnik Y., Polekhovskiy Y.P., Shilovskikh V.V., Zaitsev A.M., Vereshchagin O.S. and Britvin S.N. (2019) Nickolayite, IMA 2018-126. CNMNC Newsletter No. 47, February 2019, page 146. *Mineralogical Magazine*, **83**, 143–147.
- Novikov I., Vapnik Ye. and Safonova I. (2013) Mud volcano origin of the Mottled Zone, Southern Levant. *Geoscience Frontiers*, **4**, 597–619.
- Oliyynyk A.O., Lomnytska Y.F., Dzevenko M.V., Stoyko S.S. and Mar A. (2013) Phase equilibria in the Mo–Fe–P System at 800 °C and structure of ternary phosphide (Mo_{1-x}Fe_x)₃P (0.10 ≤ x ≤ 0.15). *Inorganic Chemistry*, **52**, 983–991.
- Pasero M. (2022) *The New IMA List of Minerals*. International Mineralogical Association, Commission on New Minerals Nomenclature and Classification (IMA-CNMNC), <http://cnmnc.main.jp/>.
- Pauling L. (1960) *The Nature of the Chemical Bond*, 3rd ed., Cornell University Press: Ithaca, New York.
- Reverdatto V.V. (1970) Pyrometamorphism of limestones and the temperature of basaltic magmas. *Lithos*, **3**, 135–143.
- Rigaku Oxford Diffraction (2021) *CrysAlisPro, Data Collection and Data Reduction GUI*. Rigaku Corporation, Tokyo, Japan.
- Rundqvist S. and Nawapong P.C. (1966) The crystal structure of ZrFeP and related compounds. *Acta Chemica Scandinavica*, **20**, 2250–2254.
- Ryb U., Erel Y., Matthews A., Avni Y., Gordon G.W. and Anbar A.D. (2009) Large molybdenum isotope variations trace subsurface fluid migration along the Dead Sea transform. *Geology*, **37**, 463–466.
- Sharygin V.V., Sokol E.V. and Vapnik Y. (2008) Minerals of the pseudobinary perovskite-brownmillerite series from combustion metamorphic larnite rocks of the Hatrurim Formation (Israel). *Russian Geology and Geophysics*, **49**, 709–726.
- Sharygin V.V., Britvin S.N., Kaminsky F.V., Wirth R., Nigmatulina E.N., Yakovlev G.A., Novoselov K.A. and Murashko M.N. (2021) Ellinaite, CaCr₂O₄, a new natural post-spinel oxide from Hatrurim Basin, Israel, and Juína kimberlite field, Brazil. *European Journal of Mineralogy*, **33**, 727–742.
- Sheldrick, G.M. (2015) Crystal structure refinement with SHELXL. *Acta Crystallographica*, **C71**, 3–8.
- Sokol E.V., Kokh S.N., Sharygin V.V., Danilovsky V.A., Seryotkin Y.V., Liferovich R., Deviatiiarova A.S., Nigmatulina E.N. and Karmanov N.S. (2019) Mineralogical diversity of Ca₂SiO₄-bearing combustion metamorphic rocks in the Hatrurim Basin: implications for storage and partitioning of elements in oil shale clinkering. *Minerals*, **9**, 465.
- Sokol E.V., Kokh S.N., Seryotkin Yu.V., Deviatiiarova A.S., Goryainov S.V., Sharygin V.V., Khoury H.N., Karmanov N.S., Danilovsky V.A. and Artemyev D.A. (2020) Ultrahigh-temperature sphalerite from Zn-Cd-Se-rich combustion metamorphic marbles, Daba complex, Central Jordan: Paragenesis, chemistry, and structure. *Minerals*, **10**, 822.
- Souza Z.S., Wang C., Jin Z.-M., Li J.-W., Yang J., Botelho N.F., Viana R.R., Santos L., Liu P.-L. and Li W. (2019) Pyrometamorphic aureoles of Cretaceous sandstones and shales by Cenozoic basic intrusions, NE Brazil: Petrographic, textural, chemical and experimental approaches. *Lithos*, **326–327**, 90–109.
- Tarkian M., Krstic S., Klaska K.-H. and Liefmann W. (1997) Rhodarsenide, (Rh,Pd)₂As, a new mineral. *European Journal of Mineralogy*, **9**, 1321–1325.
- Vapnik Ye., Sharygin V., Sokol E. and Shagam R. (2007) Paralavas in a combustion metamorphic complex, Hatrurim Basin, Israel. *GSA Reviews in Engineering Geology*, **18**, 33–153.
- Zolensky M.E., Gounelle M., Mikouchi T., Ohsumi K., Le L., Hagiya K. and Tachikawa O. (2008) Andreyivanovite: a second new phosphide from the Kaidun meteorite, *American Mineralogist*, **93**, 1295–1299.